Biosensors and Bioelectronics 126 (2019) 824–830

Contents lists available at ScienceDirect

Biosensors and Bioelectronics

journal homepage: www.elsevier.com/locate/bios

Development of dual-color total internal reflection fluorescence biosensor for simultaneous quantitation of two small molecules and their affinity constants with antibodies

Dan Song[a], Rong Yang[a], Hongliang Wang[a], Sunyan Fang[a], Yanping Liu[a], Feng Long[a,*], Anna Zhu[b,c,**]

[a] School of Environment and Natural Resource, Renmin University of China, 100872 Beijing, China
[b] Research Institute of Chemical Defense, Academy of Military Sciences PLA China, Beijing 102205, China
[c] State Key Laboratory of NBC Protection FOR Civilian, Beijing 102205, China

ARTICLE INFO

Keywords:
Dual-color fluorescence
Total internal reflection
Biosensor
Small molecule
Affinity constant

ABSTRACT

A novel dual-color total internal reflection fluorescence biosensor (DTB) was successfully developed for the simultaneous detection of two small molecules based on a simple optical structure and the time resolved effect of fiber optic switch. The DTB employed a single-multi mode fiber optic coupler instead of a sophisticated confocal optical system for the transmission of two excitation lights and dual-color fluorescence, and a photodiode detector instead of photomultiplier for the simultaneous detection of dual-color fluorescence. The compact optical design of DTB improved its optical transmission efficiency and detection sensitivity because of no requirement of numerous optical separation elements and rigorous optical alignment. The DTB was applied for the simultaneous detection of 2,4-Bisphenol-A (BPA) and 2,4-Dichlorophenoxyacetic acid (2,4-D) using one bifunctional fiber optic bio-probe modified by two hapten-protein conjugates. When the mixture of Cy5.5 labeled anti-2,4-D antibody and Pacific Blue dye labeled anti-BPA antibody was introduced over the surface of the bio-probe, they bound with their respective hapten-protein conjugate immobilized onto the bio-probe. Based on the time-resolved effect of fiber optic switch, two fluorescence dyes were alternatively excited by 635 nm and 405 nm laser lights and simultaneously detected by one photodiode detector. Taking indirect competitive immunoassay principle, BPA and 2,4-D were simultaneously detected using the DTB with high sensitivity, accuracy, and rapidity. The quantitation of affinity constants between small molecules and their antibodies was also achieved based on the proposed theory. The DTB provides a flexible and powerful platform for simultaneously sensitive quantitation of multiple targets and the affinity constants of biomolecular interactions.

1. Introduction

Simultaneous quantitative assay of multiple small molecules and their binding kinetics with antibodies from a single sample is highly desirable in the biological, medical, environmental, and chemical fields. This not only improves analysis efficiency and obtains more useful information between biomolecular interactions, but also reduces the use of precious reagents and shortens the assay period (Ewald et al., 2015; Hu et al., 2014; Li et al., 2016; Xia et al., 2017). Total internal reflect fluorescence (TIRF)-based biosensor is one of the most attractive platforms for the analysis of multiple targets (Tschmelak et al., 2006; Mondal and Hess, 2017; Ma et al., 2016; Chakkarapani et al., 2016). When the excited light transmits in the optical waveguide, the evanescent wave generates on the optical waveguide surface based on TIR principle and its typical effective penetration depth is from 100 nm to approximately a wavelength (Taitt et al., 2016; Chang et al., 2016; Long et al., 2008; Guo et al., 2018). This narrow and optically defined depth enables optical interactions between the optical waveguide and biomolecules immobilized onto its surface, minimizes background signal, and improves the resolution of TIRF detection/imaging (Qiu et al., 2016; Xiong et al., 2017; Liang et al., 2016; Rascher et al., 2014). Therefore, the TIRF technique has been widely applied for medical diagnosis, environmental monitoring, drug development, and real-time dynamics analysis of biomolecules at solid/solution interface (Long et al., 2010; Mondal and Hess, 2017; Ma et al., 2016; Chakkarapani et al., 2016; Rascher et al., 2014).

* Corresponding author at: School of Environment and Natural Resource, Renmin University of China, 100872 Beijing, China.
** Corresponding author at: Research Institute of Chemical Defense, Academy of Military Sciences PLA China, Beijing 102205, China.
E-mail addresses: longf04@ruc.edu.cn (F. Long), chuanna0306@163.com (A. Zhu).

https://doi.org/10.1016/j.bios.2018.12.010

Available online 13 December 2018
0956-5663/

Two main strategies were applied to extend the TIRF-based biosensor into the simultaneous detection of multiple targets. One strategy was that the multiple TIRF sites formed at an optical waveguide surface when a single excited light source transmitted in the optical waveguide based on TIR principle, and each of them modified by biorecognition molecules was regarded as a biosensor (Fu et al., 2016; Liu et al., 2018; Dongre et al., 2010). The fluorescence of each TIR sites was collected by optical detector (e.g. photomultiplier) to achieve the detection of multiple targets. However, their optical systems were complex, inflexible, and required sophisticated and rigorous optical design. Moreover, the fluorescence signals in various TIR sites needed a complicated optical structure and software system for identifying because of the cross-talk of fluorescence signals. The other strategy was that the multiple wavelength light sources were applied to excite multi-wavelength fluorescence dyes to achieve simultaneous detection of multiple targets (Kim et al., 2007; Rossand Dixit, 2010; Li et al., 2016). Several dual-color TIRF devices had been developed, in which two overlapping evanescent fields were generated for simultaneous detection of dual-color fluorescence (Kang et al., 2007; Leutenegger et al., 2007; Lee et al., 2008; Trexler and Taraska, 2017). These dual-color TIRF systems had emerged as powerful tools to study the binding interaction or simultaneous detection of two targets using two wavelength fluorescence probes. However, these systems were generally conducted based on the bulky bench-top optic instruments (e.g. confocal optical system). More importantly, the uniformity of the overlapped evanescent spots was difficult to achieve, and non-uniformity of evanescent field limited the simultaneous detection of different wavelength fluorescence molecules. We previously developed a fiber optic-based immunoarray biosensor to achieve simultaneous detection of two small molecules using one optic fiber bio-probe modified by two hapten-protein conjugates (Long et al., 2010). Unfortunately, it used two kinds of bandpass filters to filter two wavelength fluorescence and a digital lock-in amplifier to detect fluorescence signals. To identify two wavelength fluorescence, two bandpass filters were alternatively used in the detection process, making it be difficult to achieve real-time binding kinetic analysis on the biosensor surface (Long et al., 2010). The use of the Lock-in amplifier led to the complication of the fluorescence signal detection system.

To address above-mentioned problems, a novel dual-color TIRF biosensor (DTB) was developed for the simultaneous detection of two small molecules through integrating a compact optical system and one photodiode detector. The optical system included two lasers with different excited wavelength (635 nm and 405 nm), a 1 × 2 fiber optical switch to control the alternate excitation of two light resources, a single-multimode fiber optic coupler (SMFC) for the transmission of two excitation lights and collection and transmission of two wavelength fluorescence, and a fiber optic bio-probe modified by two hapten-protein conjugates for the simultaneous detection of two small molecules. Instead of using lock-in amplifier, one low-cost Si-based photodiode detector (SOP-1000, Beijing Reliance Co., China) was used to detect two wavelength fluorescence signals based on the time-resolved effect of the fiber optic switch. Although the fiber optic switches had been widely applied in the field of optic communication (Xie et al., 2014), they were at the first time used in the dual-color TIRF biosensor. To verify the feasibility of our proposed DTB, two small molecules, Bisphenol-A (BPA) and 2,4-Dichlorophenoxyacetic acid (2,4-D), were taken as examples. Two hapten-protein conjugates were simultaneously immobilized onto one fiber optic bio-probe as biorecognition molecules. Two fluorescence-labeled antibodies, Pacific Blue dye (PB) labeled anti-BPA antibody and Cy5.5 labeled anti-2,4-D antibody, were used as reporter molecules. Two small molecules were simultaneously detected using the DTB with high sensitivity, specificity, rapidity, reusability, cost-effectiveness, and accuracy. The affinity constants between two small molecules with their respective antibodies were also determined based on the proposed theory.

2. Experimental

2.1. Materials and reagents

BPA, 2,4-D, Bovine serum albumin (BSA), 3-mercaptopropyl-trimethoxysilane (MTS), Methylbenzene, N-(4-Maleimidobutyryloxy) succinimide (GMBS), Cy5.5 and PB were purchased from Sigma-Aldrich (Steinheim, Germany). Unless specified, all other reagents, supplied by Beijing Chemical Agents, were of analytical grade and used without further purification. Distilled deionized water was used throughout the investigation. 0.01 M phosphate buffer solution (PBS, pH = 7.4) was used. 0.5% sodium dodecyl sulfate (SDS, pH = 1.9) was applied to regenerate the bio-probe.

The monoclonal antibodies (anti-BPA antibody and anti-2,4-D antibody) and hapten-carrier proteins (BPA-OVA and 2,4-D-OVA) were produced by our research group. The anti-BPA antibodies and anti-2,4-D antibodies were labeled with PB and Cy5.5, respectively. 100 μg/mL BPA stock solutions and 100 μg/mL 2,4-D stock solutions were prepared in methanol and stored at 4 °C, respectively. Analyte standard solutions of various concentrations was prepared by serial dilutions of stock solution with PBS.

2.2. Design of the dual-color TIRF biosensor (DTB)

Fig. 1 summarized the layout and key elements of the DTB system and its photo was shown in Fig. S1. Two lasers (405 nm and 635 nm,10 mW) were selected as excitation light sources because of their monochrome, stability and compactness, and they were respectively connected with two input ports of the 1 × 2 fiber optic switch. To simplify optical structure, a SMFC was employed for transmission of two excitation lights and collection and transmission of two wavelength fluorescent signals. The single mode fiber of SMFC was linked with the output port of the fiber optic switch, and the multi-mode fiber (the ϕ 600 μm, NA = 0.22) of SMFC was connected with the proximal end of fiber optic bio-probe. The diameter of the multi-mode fiber of the SMFC was the same as that of bio-probe. The use of the SMFC reduced the required optical components (e.g. lens, dichroic mirror) and rigorous optical alignment, which decreased the optical loss originated from various optical components (Long et al., 2008). This optical design greatly improved the transmission efficiency of the excitation light and fluorescence, thus increasing the sensitivity of the DTB. Under the control of fiber optic switch, two wavelength laser beams were alternatively introduced into the single-mode fiber of the SMFC. Then, the laser light coupled into the multi-mode fiber of the SMFC from single-

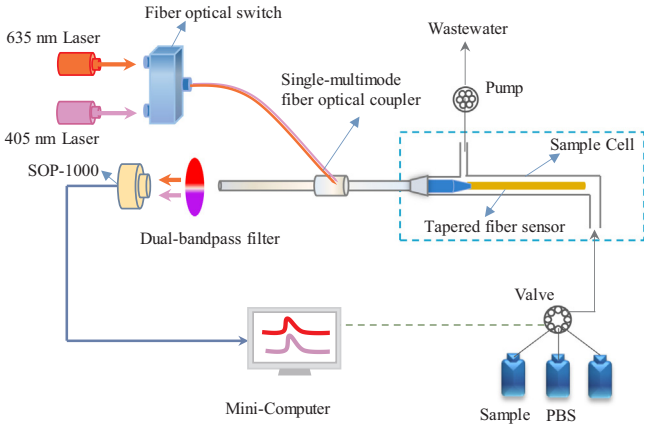

Fig. 1. Schematic diagram of the DTB system. The elegantly simplified DTB system utilizes the innovative incorporation of dual wavelength excitation coupled with fiber optic switching, which results in a powerful method to simultaneously quantify two analytes.

mode fiber and an about 3.0 mW output was obtained from the distal end of the multi-mode fiber. When the excited lights were introduced into the fiber optical bio-probe after passing the SMFC, the evanescent wave, generated on the bio-probe surface, could excite the fluorescence labeled analyte complexes bound to the bio-probe surface through binding reaction. In the DTB, two fluorescence molecules within the effective range of evanescent wave could alternatively be excited by 405 nm and 635 nm lasers, respectively. Part of fluorescence, coupled back into the fiber optical bio-probe, was detected by SOP-1000 through the collection and transmission of the multimode fiber optic of SMFC. A dual-wavelength narrow band filter (Edmundoptics, US) was used to prevent cross-talk and reject scattered excited lights, in which the two wavelengths emission fluorescence (Cy5.5 and PB) could pass through the filter. Two fluorescence signals could simultaneously be detected by the SOP-1000 based on the time resolved effect of the fiber optical switch.

The combined tapered fiber optic bio-probe was embedded in a microfluidic cell made of glass with nominal dimension of the flow channel of length 35 mm and diameter 600 μm. The fluids (e.g. samples, buffer) in the DTB system was pumped into the sample cell by a six-roller peristaltic pump. The type of input fluid medium was selected by a multi-position solenoid valve (VICI Valco, Interchim) with six inlet ports and one outlet port. Both pump and valve were controlled via an RS232 port on a computer interface through a programmed procedure. The whole detection process, including baseline detection, sample assay, and regeneration, could be programmed via a user interface. The dual-color fluorescence signal traces were on-time recorded in the mini-computer.

2.3. Functionalization of fiber optic bio-probe using two hapten-protein conjugates

To simultaneously detect two small molecules, the bio-probe was functionalized with two hapten-protein conjugates (BPA-OVA and 2,4-D-OVA) according to the previous method (Long et al., 2010). First, a combined tapered fiber optic bio-probe was obtained by tube-etching method using HF acid. The effective length of the bio-probe for the sensing section was 30.0 mm. Second, the bio-probe was initially cleaned with Piranha reagents (H_2SO_4/H_2O_2, 3:1), rinsed with distilled deionized water, and dried in N_2. Then, the bio-probe was placed in 2% MTS in toluene for 2 h, rinsed with toluene, and dry in N_2. After this, it was immersed in heterobifunctional crosslinker solution (0.02 M GMBS in ethanol) for 1 h to react with thiol group in silane. Third, the bio-probe was functionalized by the mixture of 1.0 mg/mL BPA-OVA and 1.0 mg/mL 2,4-D-OVA for 2 h after rinsed with ethanol and PBS. Two hapten-protein conjugates covalently attached to the bio-probe surface, and this bifunctional bio-probe could be used to simultaneously detect BPA and 2,4-D. Finally, the fiber optic bio-probe was immersed in 2.0 mg/mL BSA for 20 min to block its non-specific adsorption sites and stored at 4 °C prior for use.

For comparison, the bio-probe modified by BPA-OVA (or 2,4-D-OVA) was also prepared according to the above method. However, the bio-probe was dipped in only containing BPA-OVA or 2,4-D-OVA solution.

2.4. Assay of affinity constant between small molecule and its antibody using DTB

To determine affinity constant between small molecule and its antibody, kinetic data are fitted to a mathematical model derived under the following assumptions: (a) the surface is homogenously covered by monolayer; (b) the immunoreaction between small molecule and antibody is first-order kinetics; (c) no interactions between binding sites exist; and (d) the amount of the antibody is far larger than that of the hapten-protein conjugate sites on the bio-probe surface (Li et al., 2008, 2009; Salimi-Moosavi et al., 2012).

Given that the concentration of antibodies is much higher than that of the antigens, the mass transport flux is much faster than the reaction rate, thus the biomolecular reaction is limited by the interaction kinetics. The binding reaction between small molecule (S) immobilized on the biosensor surface and antibody (A) in solution can be described by

$$S + A \underset{k_{off}}{\overset{k_{on}}{\rightleftharpoons}} \text{S·A} \tag{1}$$

where the formation and dissociation of an affinity complex, S·A, between small molecule and its antibody, are characterized by rate constants k_{on} and k_{off} of the forward and reverse processes, respectively. The stability of the complex is described in terms of the equilibrium affinity constant $K_a = k_{on}/k_{off}$.

The rate equation for binding kinetics between the small molecule immobilized onto the biosensor surface and fluorescence-labeled antibody can be written as,

$$\frac{\partial [S \bullet A]}{\partial t} = k_{on}[S]_0[A]_0 - (k_{on}[A]_0 + k_{off})[S \bullet A] \tag{2}$$

At the outset of binding reaction, the forward rate is at the maximum, and the reverse rate and [S·A] are zero. [S·A] is the time-dependent concentration of the small molecule/antibody complex, $[A]_0$ is the initial concentration of the antibody, and $[S]_0$ is the surface concentration of the small molecule, averaged over the biosensor surface. When the reaction is under quasi-steady-state approximation, d[S·A]/dt = 0, and Eq. (2) gives the expression as,

$$[S \bullet A]_{eq} = \left(\frac{1}{K_a[A]_0} + 1\right)^{-1}[S]_0 \tag{3}$$

Then, we can get,

$$\frac{1}{[S \bullet A]_{eq}} = \frac{1}{K_a[S]_0} \bullet \frac{1}{[A]_0} + \frac{1}{[S]_0} \tag{4}$$

Because the intensity of the fluorescence signal of the measurement is proportional to the small molecule-antibody complex, the Eq. (4) can be written as,

$$\frac{1}{I_{eq}} = \frac{1}{K_a I_{max}} \bullet \frac{1}{[A]_0} + \frac{1}{I_{max}} \tag{5}$$

where I_{eq} is the fluorescence intensity when a balance state was obtained at a certain concentration of fluorescence-labeled antibody; I_{max} is the maximum fluorescence intensity when all binding sites of the biosensor surface are occupied by fluorescence-labeled antibody. As shown in Eq. (5), perfect data will yield a straight line of slope $\frac{1}{K_a I_{max}}$ and an x-intercept of $\frac{1}{I_{max}}$. If various concentrations of fluorescence-labeled antibodies are tested, the equilibrium affinity constant K_a can be obtained.

3. Results and discussion

3.1. Characterization of the DTB

To verify the ability of the DTB for the simultaneous detection of two small molecules, the bifunctional bio-probe modified by BPA-OVA and 2,4-D-OVA was embedded in the sample cell. When no fluorescence labeled antibody was introduced into the sample, two signal baselines were shown in the DTB user interface (Fig. 2). Then, several control experiments were performed as following. First, when 2.0 μg/mL PB-anti-BPA antibody was introduced into the sample cell, the black signal trace (as Signal channel 1) increased over the time. This indicated that the PB-anti-BPA antibody bound with the BPA-OVA immobilized onto the bio-probe surface and was excited by evanescent wave originated from 405 nm excitation light. However, the red signal trace (as Signal channel 2) was unchanged. After regenerated by SDS solution, the black

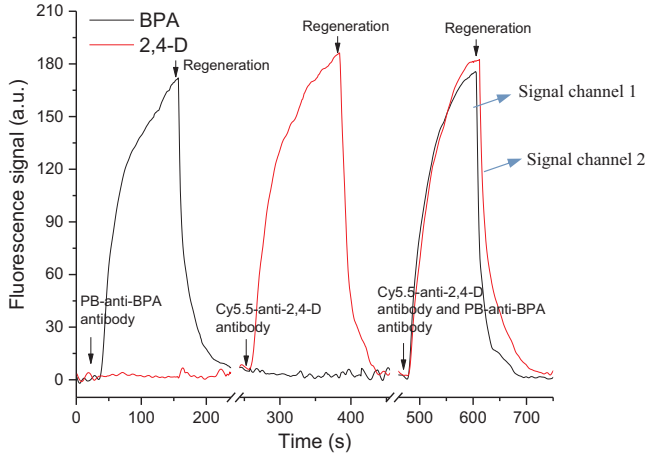

Fig. 2. The DTB system enables simultaneously measuring the response of the two different analytes (1.0 μg/mL Cy5.5-anti-2,4-D antibody and 2.0 μg/mL PB-anti-BPA antibody) with negligible interference from each other.

signal trace decreased rapidly over the time and came back to the baseline. Second, when 1.0 μg/mL Cy5.5-anti-2,4-D antibody was introduced into the sample cell, the signal channel 2 increased over the time. This indicated that the Cy5.5-anti-2,4-D antibody bound with the 2,4-D-OVA immobilized onto the bio-probe surface and was excited by evanescent wave originated from 635 nm excitation light. However, the signal channel 1 was unchanged. The signal channel 2 could also come back to the baseline after regeneration. Third, when the mixture of PB-anti-BPA antibody and Cy5.5-anti-2,4-D antibody was pumped into the sample cell, two signal channels increased over the time. Two wavelength fluorescence signals were simultaneously detected on time by the SOP-1000, which could easily discriminate two wavelength fluorescence signals using the time-resolved effect of the fiber optical switch. The fluorescence intensity of two signal channels was almost similar as that of single fluorescence-labeled antibody added into the sample cell. Then, two signal trace came back to the baseline after regeneration. These results confirmed that the two hapten-protein conjugates were successfully immobilized onto the bio-probe, and the observed fluorescence signals of two signal channels originated from the fluorescence-labeled antibodies specifically bound with their respective hapten-protein conjugates. The cross-talk of fluorescence signals of two signal channels and the cross-reactivity of two antibodies was negligible. Therefore, the DTB could be used for the simultaneous detection of two targets.

Furthermore, we compared the performance of the bifunctional bio-probe to that of the bio-probe modified by one hapten-protein conjugate. Taking 2,4-D-OVA modified fiber optic bio-probe for example, the fluorescence intensity of the bifunctional bio-probe was lower than that of 2,4-D-OVA modified bio-probe (Fig. S2) when the concentration of anti-2.4-D antibody was the same. This should contribute to the less 2,4-D-OVA immobilized onto the bifunctional bio-probe due to the occupation of part coordination sites in the bifunctional bio-probe surface by BPA-OVA. Although a reasonable fluorescence intensity was necessary to generate a good signal-to-noise ratio (SNR), the sensitivity of biosensor was also essential for the view of practical applications. Herein, a sensitivity index was introduced to determine the performance of two kinds of bio-probes as following.

$$\varepsilon = \frac{F_b - F_s}{F_b} \quad (6)$$

where F_b and F_s are the fluorescence intensities of the immunoassay without targets and with targets of a certain concentration, respectively. The mixture of Cy5.5-anti-2,4-D antibody and 1.0 μg/mL 2,4-D solution was introduced into the two kinds of bio-probe surfaces, the fluorescence intensity of the bifunctional bio-probe was lower than that of 2,4-D-OVA modified bio-probe. However, the sensitivity index (0.49) of the former was higher than that of the later (ε = 0.32) (Fig. S2). This demonstrated that the bifunctional bio-probe was conducive to the competitive binding between fluorescence-labeled anti-2,4-D antibody and 2,4-D in sample solution because the less 2,4-D-OVA was immobilized onto the bio-probe surface. Actually, the BPA-OVA modified bio-probe had the similar results (Fig. S2). The sensitivity index (ε = 0.44) of the bifunctional bio-probe was higher than that of BPA-OVA modified bio-probe (ε = 0.37).

Furthermore, a good regeneration performance of the immunosensing surface was also a desired feature for immunosensors. After each determination cycle, two kinds of non-covalently bound antibodies on the bifunctional bio-probe surface could be completely removed and the active immunosensing surface was regenerated using 0.5% SDS solution (Fig. 2). As our previous results (Long et al., 2010; Zhou et al., 2016), the hapten-protein conjugates modified immunosensor could be reused more than 100 times without signification loss of activity (Fig. S3). All results indicated that the proposed DTB platform was suitable to be used for the surface-based immunoassay of two small molecules.

3.2. Simultaneous immunoassay mechanism for two small molecules

The indirect competitive binding inhibition mechanism was employed for simultaneous determination of 2,4-D and BPA (Fig. 3A). Fig. 3B shown the typical binding curves of two signal channels. One analysis cycle had four steps as followings. First, the bifunctional bio-probe modified by 2,4-D-OVA and BPA-OVA was embedded in the

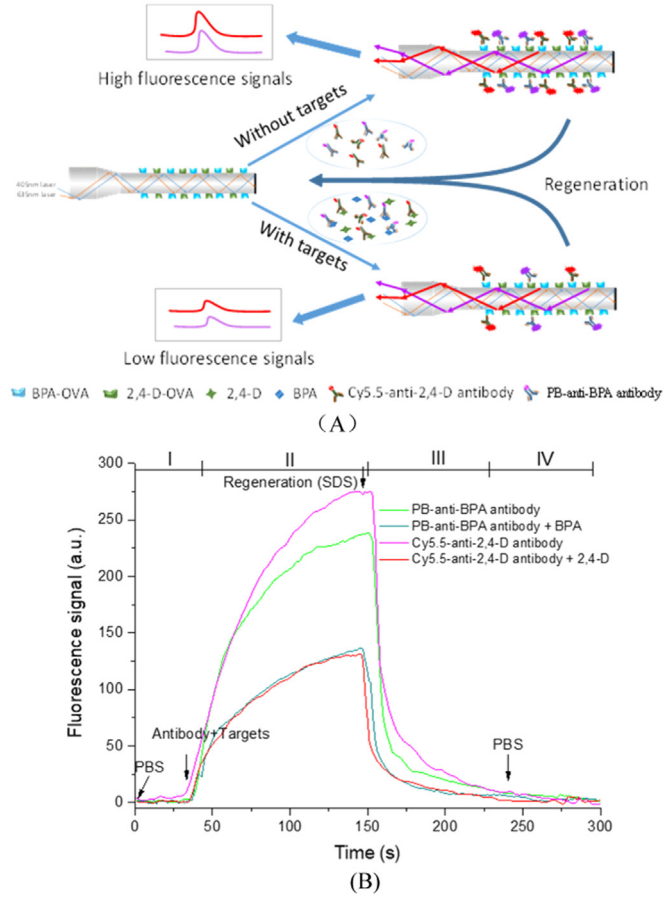

Fig. 3. (A) Schematic of simultaneous immunoassay mechanism of two small molecules (BPA and 2,4-D) based on the DTB. (B) The DTB exhibits a good performance for the simultaneous detection of 2,4-D and BPA (Cy5.5-anti-2,4-D antibody and PB-anti-BPA antibody were 2.0 μg/mL and 3.0 μg/mL, respectively; the concentration of 2,4-D and BPA was 1.0 μg/L).

sample cell, and Phase I in Fig. 3B shown the baseline of two signal channels after PBS solution was introduced. Second, the samples containing two small molecules of various concentrations were pre-reacted with a certain concentration of fluorescence-labeled anti-2,4-D antibody and anti-BPA antibody for 5 min. During this process, part of two fluorescence-labeled antibodies specifically bound with their respective targets, and the occupied antibody binding sites were proportional to the concentration of targets in the samples. Then, the mixture was introduced into the sample cell, the fluorescence signals of two signal channels initially rapidly increased over time (Phase II in Fig. 3B). This increase indicated that two fluorescence labeled antibodies containing free binding sites specifically bound to the their respective hapten-protein conjugates on the bifunctional bio-probe. Because the 405 nm and 635 nm excitation lights were alternatively introduced into the bio-probe, both Cy5.5-anti-2,4-D antibody and PB-anti-BPA antibody bound onto the bio-probe surface were alternatively excited by evanescent waves generated from 405 nm and 635 nm excitation lights, respectively. Two wavelength fluorescence signals were simultaneously detected by DTB based on the time-resolved effect of the fiber optical switch. Third, after each detection cycle, 0.5% SDS solution (pH = 1.9) was pumped over the bio-probe surface (Phase III in Fig. 3B), the fluorescence signals of two signal channels rapidly decreased because the regeneration solution broke the association between antibodies and hapten-protein conjugates. Finally, PBS solution was used to completely remove the fluorescence labeled antibodies (Phase IV in Fig. 3B). The whole detection process, including pre-reaction, detection, and regeneration, was only 10 min.

When the mixture of two fluorescence labeled antibodies and two small molecules was added into the sample cell, the fluorescence signals of two signal channels also increased, which were lower than those of the blank samples without 2,4-D and BPA (Fig. 3B). This was because part binding sites of two antibodies was occupied by their respective targets in sample, resulting in the less fluorescence labeled antibodies bound to the hapten-protein conjugates immobilized onto the bio-probe surface. Therefore, the lower fluorescence signals were detected.

3.3. Simultaneous detection of two small molecules using DTB

To obtain the dose-response curves of 2,4-D and BPA, a fixed concentration of antibodies (2.0 μg/mL Cy5.5-anti-2,4-D antibody and 3.0 μg/mL PB-anti-BPA antibody) were pre-reacted with the samples containing 2,4-D and BPA of various concentrations in the range of 0–1000 μg/L for 5 min. Then, the mixture was introduced into the sample cell. Typical time-dependent traces recorded by the DTB were shown in Fig. 4(A, B). The fluorescence signals decreased with increasing the concentration of 2,4-D and BPA in the samples. For each assay, the net fluorescence intensity *(I)* for the subsequent determination of dose-response relationships were calculated by subtracting the baseline signal value according to Eq. (7):

$$I = \text{Signal value after the 100 s reaction} - \text{Signal value at the baseline} \quad (7)$$

The normalized response was calculated according to Eq. (8):

$$I_n = \Delta I / I_b = (I_b - I_s)/I_b \text{(a. u. fluorescence intensity)} \quad (8)$$

where, I_b is the net fluorescent intensity of the blank in the absence of 2,4-D and BPA, and I_s is the net fluorescent intensity of the samples in the presence of 2,4-D and BPA.

The dose-response curve for 2,4-D or BPA detection was normalized by expressing the fluorescence intensity of each standard point as the ratio to the fluorescence intensity of the blank sample containing no 2,4-D or BPA according to Eq. (8), respectively. The dose-responses of 2,4-D and BPA were demonstrated in Fig. 4C, which were plotted against the logarithm of the concentration of 2,4-D or BPA using a four-parameter logistic equation (Supporting information). The error bars in the Fig. 4C corresponded to the standard deviation of the data points in

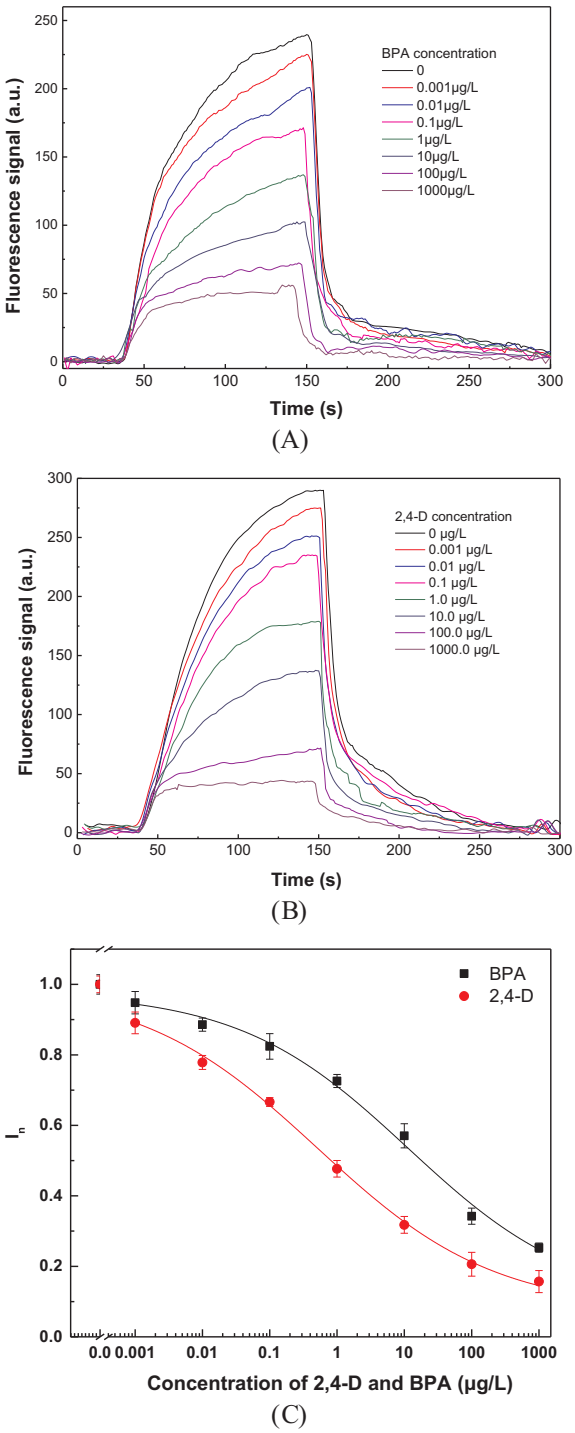

Fig. 4. The DTB allows simultaneously quantifying two small molecules based on indirect competitive immunoassay principle. (A) Typical signal curves of BPA detection using the DTB (3.0 μg/mL anti-BPA antibody); (B) Typical signal curves of 2,4-D detection using the DTB (2.0 μg/mL anti-2,4-D antibody); (C) Dose-response curve of 2,4-D and BPA detection based on bifunctional bio-probe. The error bars corresponded to the standard deviation of the data points in three repeated experiments (n = 3).

triplicate experiments, and all of them were less than 3.6%, indicating that the good stability of DTB for simultaneous detection of two small molecules. From Fig. 4C, the limit of detection (LODs) determined for BPA and 2,4-D using three times standard deviation of the mean blank values were 0.0068 μg/L and 0.0032 μg/L, respectively. The linear response of BPA and 2,4-D ranged from 0.017 μg/L to 122.26 μg/L and

from 0.009 μg/L to 101.0 μg/L, respectively. These were lower than those LODs of BPA and 2,4-D obtained using single hapten-protein conjugate modified bio-probe in our previous researches (Long et al., 2014; long et al., 2008). That the sensitivity of the bifunctional bio-probe was higher than that of single hapten-protein conjugate modified bio-probe should contribute to the higher sensitivity index of the former. Furthermore, the high sensitivity of the DTB for 2,4-D and BPA detection was also highly comparable to other immunoassay methods (Table S1). Therefore, the DTB could simultaneously detect two small molecules with high sensitivity and rapidity because of the high fluorescence collection efficiency and good time-resolved effect of the fiber optic switch.

To evaluate the ability of the DTB to simultaneously detect two small molecules in real samples, the recovery experiments of 2,4-D and BPA at different concentrations were carried out with spiked water samples using lab tap water and commercially available bottled water. These water samples were spiked with 2,4-D and BPA from their stock solution at concentrations of 0.1, 1.0, and 10.0 μg/L. Table S2 demonstrated that the 2,4-D and BPA recoveries in the spiked samples were in the range of 79.0–110.0% and 84.4–110.0%, and the relative standard deviations were less than 10.1% and 10.2%, respectively. These results indicated that the proposed method was capable of detecting 2,4-D and BPA in real water samples, and the interference from real water samples was negligible.

3.4. kinetics analysis of antibody/antigen interactions

Understanding the interactions between small molecules and proteins was greatly important for the advancement of basic science, drug discovery, medical diagnosis, and biosensor development. Affinity-based methods were the most common approach to elucidate biomolecular interactions (e.g. small molecule and protein, protein and protein, DNA and protein). Herein, the DTB was applied to investigate the affinity constants between small molecules and their respective antibodies.

To evaluate the affinity constant of the immunocomplex of anti-small molecule antibodies with small molecules, fluorescence labeled antibody of various concentrations (from 1.0 μg/mL to 10.0 μg/mL) were introduced into the sample cell and the fluorescence intensity was measured. The relationship between the antibody concentration and the fluorescence intensity was shown in Fig. 5A. From Fig. 5A, when the mixture of Cy5.5-anti-2,4-D antibody and PB-anti-BPA antibody was introduced over the bifunctional bio-probe, the fluorescence intensities of two signal channels were almost the same as that obtained by Cy5.5-anti-2,4-D antibody (or PB-anti-BPA antibody). This indicated that the coexistence of the two antibodies did not affect their binding reaction with their respective hapten-protein conjugates. Plots summarizing the concentration-dependent anti-small molecule antibody binding to hapten-protein conjugates exhibited characteristic linear response at low concentrations and saturation at higher concentrations (Fig. 5A). According to Eq. (5), $1/I_{eq}$ was plotted against $1/[A]_0$ as shown in Fig. 5(B, C). Good linear relationships between $1/I_{eq}$ and $1/[A]_0$ for two small molecules and their respective antibodies were obtained, indicating that the first-order kinetics held. When the mixture of Cy5.5-anti-2,4-D antibody and PB-anti-BPA antibody were added, the affinity constants between BPA and 2,4-D and their respective antibodies were determined as and $6.99 \times 10^8\ M^{-1}$ and $6.15 \times 10^8\ M^{-1}$, respectively. These affinity constants were almost similar with those determined by single anti-small molecule antibody introduced into the bio-probe, in which the affinity constants of BPA and 2,4-D were $7.75 \times 10^8\ M^{-1}$ and $7.01 \times 10^8\ M^{-1}$, respectively. This indicated that the binding kinetics between two small molecules and their respective antibodies did not affect each other, which should contribute to the few cross-reactivity between anti-2,4-D antibody and anti-BPA antibody. These results demonstrated that the DTB could serve as a simple and potentially quantitative assay platform for binding kinetics between small

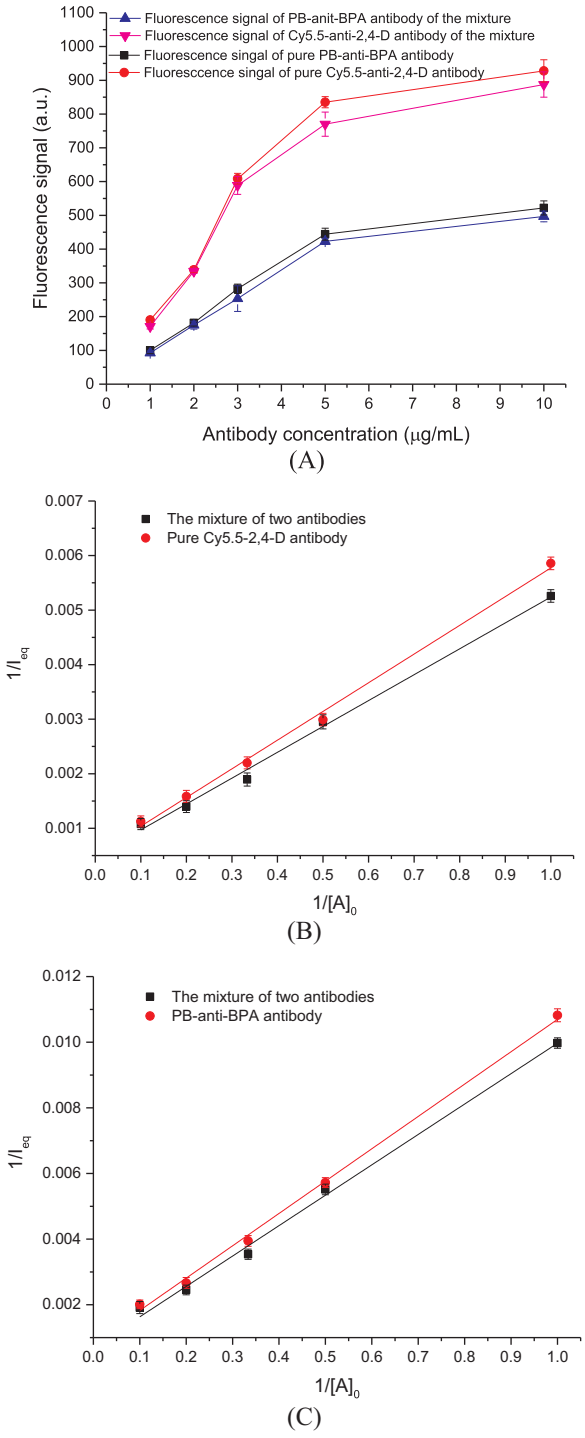

Fig. 5. The DTB serves as a quantitative assay platform for binding kinetics between small molecules and their antibodies. (A) Fluorescence signals of pure Cy5.5-anti-2,4-D antibody, pure PB-anti-BPA antibody, or the mixture of two antibodies at various concentrations (1.0, 2.0, 3.0, 5.0, and 10.0 μg/mL) was detected by bifunctional bio-probe. (B) Dependence of $1/I_{eq}$ against $1/[A]_0$ for the association between Cy5.5-anti-2,4-D antibody and 2,4-D when pure Cy5.5-anti-2,4-D antibody or the mixture of two antibodies was introduced over the bifunctional bio-probe. (C) Dependence of $1/I_{eq}$ against $1/[A]_0$ for the association between PB-anti-BPA antibody and BPA when pure PB-anti-BPA antibody or the mixture of two antibodies was introduced over the bifunctional bio-probe. The error bars corresponded to the standard deviation of the data points in three repeated experiments (n = 3).

molecules and proteins.

4. Conclusions

In summary, a novel dual-color TIRF biosensor (DTB) was developed for the simultaneous detection of two targets through integrating a simple and compact optical structure and one photodiode detector. The DTB could detect two wavelength fluorescence signals by a single photodiode detector based on the time-resolve effect of the optic fiber switch. Using a bifunctional bio-probe, the simultaneous immunoassay of BPA and 2,4-D was performed by the DTB with high sensitivity, accuracy, and rapidity. The quantitation of affinity constants of between small molecules and their antibodies was also achieved using the DTB based on the proposed theory. Compared with other dual-color fluorescence detection system, the DTB had several advantages as followings. First, in the DTB system, a single-multi mode fiber optic coupler instead of a sophisticated confocal optical system was employed for the transmission of two excitation lights and the collection and transmission of dual-color fluorescence. Therefore, the requirement of numerous optical separated elements and rigorous optical alignment was unnecessary. Moreover, a photodiode detector instead of photomultiplier for the simultaneous detection of dual-color fluorescence based on the time-resolved effect of the fiber optic switch. The simple and compact optical design of DTB improved its optical transmission efficiency and detection sensitivity. Second, using a bifunctional bio-probe modified by two hapten-protein conjugates, two completely overlapping evanescent fields were generated for simultaneous detection of dual-color fluorescence when two excitation lights were alternatively introduced into the bio-probe based on the time-resolved effect of the optic fiber switch. This allowed the DTB to be a powerful tool for mapping various binding affinities between various biomolecular interactions including small molecule-protein, DNA-protein, and protein-protein. Third, based on indirect competitive immunoassay principle, two targets (e.g. BPA and 2,4-D) could be simultaneously detected using the DTB with high sensitivity and rapidity. The whole detection process, including pre-reaction, detection, and regeneration, was only 10 min. In addition, The DTB in the spiked water samples showed good recovery, precision, and accuracy. The proposed DTB system can be readily extended toward the sensitive and rapid detection of multiple targets in the environmental, medical, and chemical field. It also provides a flexible and powerful platform for simultaneous quantitation of the affinity constants between various biomolecular interactions.

Acknowledgements

This work was supported by the National Natural Science Foundation of China (21675171, 21277173); the National Instrument Major Project of China (2012YQ3011105); and the Special Fund of State Key Joint Laboratory of Environment Simulation and Pollution Control (17K06ESPCT).

Declaration of interests

None.

Appendix A. Supplementary material

Supplementary data associated with this article can be found in the online version at https://doi.org/10.1016/j.bios.2018.12.010

References

Chakkarapani, S.K., Zhang, P., Ahn, S., Kang, S.H., 2016. Biosens. Bioelectron. 81, 23–31.
Chang, Y.F., Fu, C., Chen, Y.T., Jou, F.J., Chen, C.C., Chou, C., Ho, J.A.A., 2016. Biosens. Bioelectron. 77, 1201–1207.
Dongre, C., Weerd, J., Bellini, N., Osellame, R., Cerullo, G., Weeghel, R., Hoekstra, J.W.M.H., Pollnau, M., 2010. Biomed. Opt. Express 1, 729–735.
Ewald, M., Fechner, P., Gauglitz, G., 2015. Anal. Bioanal. Chem. 407, 4005–4013.
Fu, Y., Winter, W.P., Rojas, R., Wang, V., McAuliffe, M., Patterson, H.G., 2016. PNAS 113, 4368–4373.
Guo, M., Chandris, P., Giannini, J.P., Trexler, A.J., Fischer, R., Chen, J., Vishwasrao, H.D., Rey-Suarez, I., Wu, Y., Waterman, C.M., Patterson, G.H., Upadhyaya, A., Taraska, J., Shroff, H., 2018. Nat. Methods. https://doi.org/10.1101/182121.
Hu, R., Liu, T., Zhang, X.B., Huan, S.Y., Wu, C., Fu, T., Tan, W., 2014. Anal. Chem. 86, 5009–5016.
Kang, S.H., Kim, Y.J., Yeung, E.S., 2007. Anal. Bioanal. Chem. 387, 2663–2671.
Kim, D., Hee, G.L., Jung, H., Seong, H.K., 2007. Bull. Korean Chem. Soc. 28, 783–790.
Lee, S., Chung, B.H., Kang, S.H., 2008. Curr. Appl. Phys. 8, 700–705.
Leutenegger, M., Hassler, K., Rigler, P., Bilenca, A., And, T.L., 2007. ACS Symp. 963, 259–279.
Li, Q., Chen, P., Fan, Y., Xu, W., Xu, K., Lu, L., Bo, T., 2016. Anal. Chem. 88, 8610–8616.
Li, Y., Kobayashi, M., Furui, K., Soh, N., Nakano, K., Imato, T., 2008. Anal. Lett. 576, 77–83.
Li, Y., Ren, J., Nakajima, H., Kim, B.K., Soh, N., Nakano, K., Imato, T., 2009. Talanta 77, 473–478.
Liang, L., Zuo, Y.F., Wu, W., Zhu, X.Q., Yang, Y., 2016. Lab Chip 16, 3007–3014.
Liu, L., Shan, D., Zhou, X., Shi, H., Song, B., Falke, F., Leinse, A., Heideman, R., 2018. Biosens. Bioelectron. 106, 117–121.
Long, F., He, M., Zhu, A.N., Song, B.D., Sheng, J.W., Shi, H.C., 2010. Biosens. Bioelectron. 26, 16–22.
Long, F., Shi, H.C., He, M., Zhu, A.N., 2008. Biosens. Bioelectron. 23, 1361–1366.
Long, F., Zhu, A., Zhou, X., Wang, H.C., Zhao, Z., Liu, L.H., 2014. Biosens. Bioelectron. 55, 19–25.
Ma, F., Liu, M., Wang, Z.Y., Zhang, C.Y., 2016. Chem. Commun. 52, 1218–1221.
Mondal, P.P., Hess, S.T., 2017. Appl. Phys. Lett. 110, e100589.
Qiu, H., Gao, S., Chen, P., Li, Z., Liu, X., Zhang, C., Xu, Y., Jiang, S., Yang, C., Huo, Y., 2016. Opt. Commun. 366, 275–281.
Rascher, D., Geerlof, A., Kremmer, E., Krämer, P., Michael, S., Hartmann, A., Rieger, M., 2014. Biosens. Bioelectron. 59, 251–258.
Ross, J.L., Dixit, R., 2010. Methods Cell Biol. 95, 521–542.
Salimi-Moosavi, H., Rathanaswami, P., Rajendran, S., Toupikov, M., Hill, J., 2012. Anal. Biochem. 426, 134–141.
Taitt, C.R., Anderson, G.P., Ligler, F.S., 2016. Biosens. Bioelectron. 76, 103–112.
Trexler, A.J., Taraska, J.W., 2017. Methods Mol. Biol. 1563, 151–165.
Tschmelak, J., Kumpf, M., Käppel, N., Proll, G., Gauglitz, G., 2006. Talanta 69, 343–350.
Xia, Y., Su, R., Huang, R., Ding, L., Wang, L., Qi, W., He, Z., 2017. Biosens. Bioelectron. 92, 266–272.
Xie, N., Hashimoto, T., Utaka, K., 2014. J. Light Technol. 32, 3067–3073.
Xiong, Y., Wu, J., Wang, Q., Xu, J., Fang, S., Chen, J., Duan, M., 2017. Talanta 174, 372–379.
Zhou, L., Zhu, A., Lou, X., Song, D., Yang, R., Shi, H., Feng, L., 2016. Anal. Chim. Acta 905, 140–148.